Seasonally apportioning the potential sources and transport pathways of atmosphere particulate matter in Hefei City, the most rapidly developing megalopolis in China

Siping Niu (sipingniu@126.com)
Anhui University of Technology
Tiantian Wang
Anhui University of Technology
Jianghua Yu
Nanjing University of Information Science & Technology

Research Article

Keywords: Particulate matter, Potential source, Backward trajectory, Transport pathway, Hefei

Posted Date: April 13th, 2022

DOI: https://doi.org/10.21203/rs.3.rs-1518822/v1

Additional Declarations: No competing interests reported.

Abstract

Trajectories cluster analysis (CA), potential source contribution function (PSCF) method and concentration weighted trajectories (CWT) method were integrated to identify the potential sources of particulate matter (PM_{10} and $PM_{2.5}$) during 2018 to 2020 in Hefei city of China. From 2018 to 2020 PM_{10} and $PM_{2.5}$ were annually averaged at 66.74 ± 33.05 $\mu g \cdot m^{-3}$ and 38.08 ± 23.05 $\mu g \cdot m^{-3}$, respectively. Correspondingly, the mean concentrations in spring, summer, autumn and winter were 73.41 ± 30.04, 45.80 ± 16.50, 72.75 ± 35.10 and 81.81 ± 38.17 $\mu g \cdot m^{-3}$ for PM_{10} while 38.73 ± 15.73, 24.26 ± 10.73, 37.16 ± 19.60 and 61.42 ± 32.16 $\mu g \cdot m^{-3}$ for $PM_{2.5}$, with the highest in winter while the lowest in summer. CA shows that Hefei's atmosphere particulate matter pollution was mainly affected by those air flows derived from the north and northwest China in spring, autumn and winter, while south and southeast during the summer. The pressures of backjectories were in the range of 700 ~ 950 hPa during four seasons, wherein summer had a higher pressure than that of other seasons. This means that the influence of near surface air mass was stronger in summer. PSCF and CWT analysis indicate that winter had the largest number of potential contribution sources. In spring, autumn and winter several cities from the Fen-Wei Plain and '2 + 26' cities were identified as the major contributor. In addition, some places in Anhui province were also the considerably potential contributor. It is found the air pollution transport pathways reaching Hefei City have changed recently. This study could benefit the prevention and control of air pollution in city clusters and metropolitan area in China.

1. Introduction

Many cities in China are facing severe air pollution resulted from economic development, population growth and urbanization [1–4]. Particulate matter (PM) pollution, represented by PM_{10} and $PM_{2.5}$, has been of great concern [5, 6], because it can not only lead to various environment problem like decreasing in atmospheric visibility and increasing in haze day and climate change but also human health impairment as respiratory and cardiovascular disease [7, 8].

Owing to the efforts on air pollution control in China, the concentrations of PM_{10} and $PM_{2.5}$ have been decreased gradually in many places [9, 10]. Nevertheless, air pollution by PM still was at unfavorable level, especially in winter [11]. For example, $PM_{2.5}$ is much higher than the specified value (10 $\mu g \cdot m^{-3}$) by WHO in almost all cities. The challenge of air pollution control is that the urban air pollution is not only affected by local pollution sources, but also related with the contribution of external sources [12, 13]. Therefore, it becomes greatly important to determine the potential sources and diffusion pathways for air quality improvement.

Statistical method like clustering analysis on air mass trajectories has been proved to be an effective method to identify the sources and prevalent transport pathways of airborne pollutants [14–15]. Trajectory clustering can sort the air-mass into representative groups based on velocity or angle of air flow. Potential sources contribution function (*PSCF*) improves the resolutions of source areas via giving high resolution data [16]. However, it is good at angular resolution but poor radial resolution because of trajectories convergence as they approach the receptor [17, 18]. These days trajectory clustering, PSCF and WCT are usually integrated to characterize the sources of atmospheric pollutant to obtain much more information [18, 19].

Hefei, one megalopolis located in East China, is the most rapidly developing city in China with the population up to ~ 9.4 million in 2020. To date, many comprehensive studies on PM in China have been concentrated at Beijing–Tianjin–Hebei Province, the Yangtze River Delta and the Pearl River Delta. However, in the Yangtze River Delta, the work has been mainly carried out towards those areas with high economic development level like Shanghai, Nanjing and Hangzhou. Previously, Luo et al. [20] investigated the sources of PM_{10} and $PM_{2.5}$ during 2014 in Hefei using backward trajectory model. As we know, due to the action of defending the blue sky, which was launched in 2017 throughout the country, the status of air pollution in China has greatly changed. Consequently, the timely study is of great importance. This study is conducted to better understand detailed transport pathways and potential sources of PM_{10} and $PM_{2.5}$ in Hefei during 2018 ~ 2020, which can help to figure out the variation in air pollution transport pathways with endpoint at the Yangtze River Delta during recent years. The result is potential to benefit the prevention and control of air pollution in city clusters and metropolitan area in China. We determined the main air mass transport pathways by using cluster analyses and press profile via backward trajectories and identified the significant seasonal sources based on hourly resolution data of PM using PSCF method and WCT method.

2. Materials And Method

2.1 Environmental monitoring data

Hourly concentrations of PM_{10} and $PM_{2.5}$ in Hefei were obtained from the Department of Ecology and Environment of Anhui Province (available at https://sthjt.ah.gov.cn/site/tpl/5371). The averaged data from 10 national monitoring sites (Luyang District, Amber Hills, Sanli Street, Yaohai District, Yaohai District, Baohe District, Binhu New District, Middle Changjing Road, Dongpu Reservoir, High-tech Zone and Pear Plaza) was officially used as the representative of air pollution in Hefei City (Fig. 1) by PM.

[Fig. 1 Location of Hefei City]

2.2 Trajectory computation

In this study, 72-hour back-trajectories arriving at the receptor (117.17E, 31.52 N [20] were computed hourly (00:00–23:00 Beijing time) using MeteoInfo map integrated with TrajStat (Version 2.4.5 downloaded from http://www.meteothink.org/). Daily meteorological data were available at “ftp://arlftp.arlhq.noaa.gov/pub/archives/gdas1/’ in the global data assimilation system from National Centers for Environmental Prediction”.

2.3 Trajectory clustering

Air trajectories can be grouped by their specific similarity like angle or speed. In this study the originated angle distance was selected to carry out trajectory clustering.

Potential source contribution function analysis

Potential source contribution function (*PSCF*) is a widely used method, identifying the potential contributor with high pollutant concentration to the receptor site. For given geographic grid cell (*i, j*), it is defined as [9] the following equation.

$$PSCF_{ij} = x_{ij}/y_{ij}$$

1

in which y_{ij} is the number of trajectory endpoint falling in grid cell (*i, j*) and x_{ij} is the number of trajectory endpoint with pollutant concentration over a threshold. Hence, threshold is the boundary between local emission and regional transmission. As the pollutant concentration was higher than the threshold, the pollution is mainly contributed by the regional transmission. In this study, the grid cell was set as 0.5×0.5° and the averaged concentrations of PM during each season were selected as the thresholds for the corresponding season [16]. In case of grid cell with few endpoints, the result of *PSCF* analysis will have uncertainty. To mitigate this uncertainty, $PSCF_{ij}$ values were multiplied by a weight coefficient (W_{ij}) to be $WPSCF_{ij}$ [17]. The values of W_{ij} were determined as follows.

$$W\left(n_{ij}\right) = \begin{cases} 1.00y_{ij} < 3n_{ave} \\ 0.701.5n_{ave} < y_{ij} \leq 3n_{ave} \\ 0.42n_{ave} < y_{ij} \leq 1.5n_{ave} \\ 0.17y_{ij} \leq n_{ave} \end{cases}$$

2

2.4 Concentration weighted trajectory analysis

Those grid cells, with sample concentrations either only slightly higher or much higher than the threshold, are likely to have the same *PSCF* value, resulting in difficulty in recognizing the moderate sources from the strong ones. Alternatively, concentration weighted trajectory (*CWT*) analysis was proposed. For *CWT*, each grid cell is given a weighted concentration by averaging the sample concentration, which is associated with trajectories that cross the grid cell, by following equation.

$$c_{ij} = \frac{k}{\sum_{k=1}^{M} \tau_{ijk}} \sum_{k=1}^{M} c_k \tau_{ijk}$$

3

where c_{ij} is the average weighted concentration in the grid cell (*i,j*), *k* is the index of the trajectory, *M* is the number of trajectories, c_k is the concentration observed on arrival of trajectory *k*, and τ_{ijk} is the retention time of trajectory *k* in the cell. Weight coefficient, used by *PSCF*, also was introduced into *CWT* to eliminate grid cells with small y_{ij} based on the criterion described by Eq. (2).

3. Results And Discussion

3.1 Characteristics of PM_{10} and $PM_{2.5}$

Daily concentraiton's fluctuation of PM_{10} and $PM_{2.5}$ in Hefei City is shown in Fig. 2. From 2018 to 2020 the annual averaged concentrations of PM_{10} and $PM_{2.5}$ were 66.74 ± 33.05 $\mu g \cdot m^{-3}$ and 38.08 ± 23.05 $\mu g \cdot m^{-3}$, respectively. Of three years, PM_{10} (58.84 ± 28.67 $\mu g \cdot m^{-3}$) and $PM_{2.5}$ (32.05 ± 18.64 $\mu g \cdot m^{-3}$) had the lowest concentrations in 2020 ($p > 0.05$). Also, the levels of PM in 2020 were either lower than or similar to the criterion as 70 $\mu g \cdot m^{-3}$ for PM_{10} and 35 $\mu g \cdot m^{-3}$ for $PM_{2.5}$ required by the Class II standard of the Chinese Ambient Air Quality Standards (GB 3095 – 2012). This means that the air quality of Hefei city has been improved considerably recently. However, the concentraion of PM_{10} was still higher than the annual average concentrations of 64 $\mu g \cdot m^{-3}$ of 168 Chinese cities in 2020 [11]. As to the ratio of $PM_{2.5}$ to PM_{10}, it did not fluctuate significantly over the study period with averages of 0.60 ± 0.71 in 2018, 0.56 ± 0.18 in 2019 and 0.57 ± 0.19 in 2020. The value of $PM_{2.5}/PM_{10}$ were lower than those, calculated with the data from [11], of Beijing (0.67), shanghai (0.78) and Tianjin (0.71), while similar to that of Nanjing (0.55) and Guangzhou (0.53).

[Fig. 2 Daily variation of particulate matter in Hefei city between 2018 and 2020]

As shown in Fig. 3 (a), between 2018 and 2020 the averaged concentrations of PM in spring, summer, autumn and winter were 73.41 ± 30.04, 45.80 ± 16.50, 72.75 ± 35.10 and 81.81 ± 38.17 $\mu g \cdot m^{-3}$ for PM_{10} while 38.73 ± 15.73, 24.26 ± 10.73, 37.16 ± 19.60 and 61.42 ± 32.16 $\mu g \cdot m^{-3}$ for $PM_{2.5}$. PM_{10} and $PM_{2.5}$ had the same seasonal concentration variation, the highest in winter while the lowest in summer. Meanwhile, the pollution level of PM_{10} and $PM_{2.5}$ in spring was nearly the same to that of autumn ($p < 0.001$).

Person correlationship analysis suggests that in Hefei city $PM_{2.5}$ was significantly related with PM_{10} ($p < 0.001$) with correlation coefficient (*r*) as 0.557 in spring, 0.822 in summer, 0.688 in autumn and 0.899 in winter. Based on the record by Shen [21] on Hefei, the values of *r* in spring, summer, autumn and winter during 2015–2017 were 0.811, 0.913, 0.925 and 0.947, respectively. It means that the relationship between PM_{10} and $PM_{2.5}$ had been weakened by a small margin. Therefore, the pollution sources contributing PM_{10} and $PM_{2.5}$ also had changed correspondingly. On the other hand, the values of $PM_{2.5}/PM_{10}$ were roughly the equivalent during spring (0.56 ± 0.19), summer (0.53 ± 0.14) and autumn

(0.53 ± 0.17) ($p > 0.05$). And the winter had the highest ratio as 0.75 ± 0.16. This indicates that the atmospheric pollution type of Hefei by PM in winter was different from other seasons.

[Fig. 3 Seasonal variation of particulate matter in Hefei city between 2018 and 2020]

[Fig. 4 Correlationship between PM_{10} and $PM_{2.5}$ with respect to season n Hefei city between 2018 and 2020]

3.2 Trajectories cluster

Trajectories were categorized into six clusters by the present study for each season (Fig. 5). And the analysis on PM corresponding to six clusters is summarized in Fig. 6 and Table 1. The pathways of air flow in summer were different from that of other seasons. The trajectories mainly came from the southern inland and the East China Sea during summer while from the north China and the northwest China in spring, autumn and winter. Comparatively, the migration pathway of air mass was the shortest in summer. Shi et al. [22] identified the seasonal trajectories reaching Hefei city during 2001 ~ 2005 and found they were mainly sourced from the northwest of Hefei city during spring, summer and winter, which was in accordance with the present study. However, the migration pathway got short during 2018–2020 regardless of season. Also, the air mass originated from Mongolia became rare.

[Fig. 5 Clusters of back trajectories of air flow for Hefei City between 2018 and 2020]

[Fig. 6 PM_{10} and $PM_{2.5}$ portioned by trajectory cluster of air flow for Hefei City between 2018 and 2020]

The air mass of trajectories in spring accounted for 15.22%, 19.72%, 23.83%, 3.72%, 18.84% and 8.67% for cluster 1 to 6, respectively. Cluster 1 (northwest→southwest) had the highest PM_{10} as 93.37 ± 39.22 $\mu g \cdot m^{-3}$, followed by cluster 4 (northwest) as 89.29 ± 44.17 $\mu g \cdot m^{-3}$ and cluster 3 (northwest→south) as 81.04 ± 41.80 $\mu g \cdot m^{-3}$. Also, cluster 1 was coupled with the highest $PM_{2.5}$ of 44.09 ± 19.11 $\mu g \cdot m^{-3}$. The levels of $PM_{2.5}$ from cluster 3 and 4 were almost the same, which was slightly smaller than that of cluster 1. In spring PM_{10} and $PM_{2.5}$ in Hefei were averaged at 73.41 and 38.73 $\mu g \cdot m^{-3}$, respectively. Concentrations of PM_{10} at cluster 1, 3 and 4 were higher than the average concentration of winter in Hefei, while $PM_{2.5}$ at cluster 1 to 5. Therefore, air mass from cluster 1, 3 and 4 is considered as the major transport pathway that PM migrating to Hefei in spring. The air mass of cluster 1 started from Fen-wei Plain and went through several cities of the “2 + 26” cities. Fen-wei Plain is one of the key prevention and control areas of air pollution in China. “2 + 26” cities are air pollution transmission channel of Beijing Tianjin Hebei region. Cluster 3 started from the east of Hubei while cluster 4 passed the north of Anhui. Both eastern Hubei and northern Anhui had a high concentration of PM. The ratios of $PM_{2.5}$ to PM_{10} associated with cluster 1, 3 and 4 were 0.47, 0.52 and 0.48, respectively. While, the trajectories in cluster 5 had the highest value of $PM_{2.5}/PM_{10}$as 0.61. Nonetheless, those trajectories had no high pollutant concentration and were not the significant pollution transport pathway.

Table 1

Statistical analysis on trajectories of air flow for each cluster in Hefei City between 2018 and 2020

Season	Cluster	NT[a]	PNT [b] (%)	PM_{10}[c] ($\mu g \cdot m^{-3}$)	$PM_{2.5}$[c] ($\mu g \cdot m^{-3}$)	$PM_{2.5}/PM_{10}$
Spring	1	1035	15.22	**93.37 ± 39.22**	**44.09 ± 19.11**	0.47
	2	1281	19.72	68.66 ± 30.62	**39.00 ± 22.52**	0.57
	3	1611	23.83	**81.04 ± 41.80**	**42.41 ± 19.23**	0.52
	4	900	13.72	**89.29 ± 44.17**	**42.77 ± 21.99**	0.48
	5	1228	18.84	66.62 ± 37.56	**40.50 ± 22.88**	0.61
	6	563	8.67	71.60 ± 52.51	30.88 ± 16.85	0.43
Summer	1	1054	15.60	**53.37 ± 21.56**	**27.44 ± 12.71**	0.51
	2	1888	28.84	44.00 ± 20.94	22.53 ± 9.43	0.51
	3	1421	21.66	**50.33 ± 21.84**	**26.19 ± 13.63**	0.52
	4	690	10.54	**48.20 ± 24.59**	23.49 ± 11.89	0.49
	5	917	14.01	**54.79 ± 27.32**	**26.67 ± 14.10**	0.49
	6	650	9.55	44.60 ± 22.38	21.67 ± 9.84	0.49
Autumn	1	279	4.32	**83.22 ± 54.70**	**43.80 ± 25.79**	0.53
	2	727	11.26	**81.01 ± 39.13**	**50.71 ± 35.39**	0.63
	3	1282	19.46	67.16 ± 33.68	33.71 ± 17.70	0.50
	4	1736	26.06	**73.61 ± 42.12**	37.08 ± 24.00	0.50
	5	1797	27.83	63.07 ± 29.05	35.30 ± 18.13	0.56
	6	715	11.07	**99.40 ± 64.29**	**42.16 ± 27.26**	0.42
Winter	1	1015	15.26	**89.18 ± 43.19**	**71.11 ± 42.86**	0.80
	2	2041	31.83	70.67 ± 43.40	59.37 ± 40.16	0.84
	3	1259	19.68	**89.97 ± 47.81**	**72.53 ± 42.14**	0.81
	4	872	13.59	71.82 ± 36.21	**70.75 ± 39.39**	0.99
	5	823	12.45	**94.75 ± 40.30**	**69.93 ± 35.48**	0.74
	6	461	7.19	70.01 ± 45.77	**70.00 ± 43.66**	1.00

Season	Cluster	NT[a]	PNT [b] (%)	PM_{10}[c] ($\mu g \cdot m^{-3}$)	$PM_{2.5}$[c] ($\mu g \cdot m^{-3}$)	$PM_{2.5}/PM_{10}$

[a], number of trajectories

[b], percentage of trajectories

[c], mean ± std

In summer, trajectory values of $PM_{2.5}/PM_{10}$ among clusters did not obviously vary with the values of ~ 0.50. There were four clusters (1(northwest→east), 3 (east-southeast), 4 (north→east) and 5 (southeast)) with PM_{10} higher than averaged summer concentration of Hefei while 3 (1,3 and 5) for $PM_{2.5}$. Cluster 1, 3 and 5 were regarded to be the predominant trajectories that simultaneously affected Hefei's PM_{10} and $PM_{2.5}$. Moreover, the trajectories from cluster 4 were also the major transport pathway that PM_{10} reached Hefei. Trajectories from clusters 1, 3, 4 and 5 had relationship with the city groups including Shanghai-Suzhou-Wuxi-Changzhou-Nanjing-Maanshan, Jiaxing-Suzhou-Wuxi-Changzhou-Nanjing-Wuhu, Chuzhou-Maanshan-Wuhu and Wenzhou-Lishui-Jinhua-Hangzhou-Huangshan-Chizhou-Tongling, respectively. However, the cluster 2 with the highest percentage of trajectory as 28.84% was not the major pathway of PM migrating to Hefei with heavy pollution.

In autumn, mean trajectory concentrations of PM_{10} and $PM_{2.5}$ were 83.22 ± 54.70 and 43.80 ± 25.79 $\mu g \cdot m^{-3}$ in cluster 1, 81.01 ± 39.13 and 50.71 ± 35.39 $\mu g \cdot m^{-3}$ cluster 2, 67.16 ± 33.68 and 33.71 ± 17.70 $\mu g \cdot m^{-3}$ cluster 3, 73.61 ± 42.12 and 37.08 ± 24.00 $\mu g \cdot m^{-3}$ cluster 4, 63.07 ± 29.05 and 35.30 ± 18.13 $\mu g \cdot m^{-3}$ cluster 5 and 99.40 ± 64.29 and 42.16 ± 27.26 $\mu g \cdot m^{-3}$ in cluster 6. As a result, cluster 1, 2, 4 and 6 had the trajectories with high PM_{10} level while cluster 1, 2 and 6 for $PM_{2.5}$. The corresponding trajectories of cluster 1, 2, 4 and 6 were observed to pass either Wei-fen plain or "2 + 26" cities. As to $PM_{2.5}/PM_{10}$, the highest was present in cluster 2 with 0.63 while the smallest from cluster 6 as 0.42.

For winter, the ratio of $PM_{2.5}/PM_{10}$ in trajectories was significantly higher than that of other seasons. Of those six clusters, cluster 4 and 6 had the highest ratio of around 1.00, while the smallest for cluster 5 as 0.74. And the ratio values of cluster 1, 2 and 3 were 0.80, 0.84 and 0.81. Trajectories of cluster 2, with the highest air mass fraction of 31.83%, were not associated with the concentrations of neither PM_{10} nor $PM_{2.5}$ higher than the mean concentration of PM in winter. The highest trajectory concentration of PM appeared at Cluster 5 for PM_{10} as 94.75 ± 40.30 $\mu g \cdot m^{-3}$ and cluster 3 for $PM_{2.5}$ as 72.53 ± 42.14 $\mu g \cdot m^{-3}$. Specifically, there were three clusters (1, 3 and 5) containing trajectories with high pollution of PM_{10} and 5 clusters (1, 3, 4, 5 and 6) for $PM_{2.5}$. In winter the air mass all passed the places (Wei-fen Plain and "2 + 26" cities) with heavy PM pollution in China.

Figure 7 demonstrates the press profiles of the air mass clustered reaching Hefei. Comparatively, air flow among seasons occurred with the minimum height in summer. In spring the trajectories in cluster 3 with the highest ratio and shortest moving distance were observed to have the smallest height, coupled with pressure of 840 ~ 950 hPa. Meanwhile, the height of those trajectories with the longest transport path changed considerably. Over summer the heights of flow masses in cluster 1 and 6 varied similarly, and decreased gradually. The initial height of trajectories from cluster 4 which had short pathway was the highest. Also those trajectories, derived from the East China Sea, of cluster 3 and 5 almost started at the same height. However, the air flows grouped into cluster 5 was increased and decreased successively as they moved. Coming to autumn, cluster 5 with the highest ratio contained the trajectories with the maximum height. And the height of trajectories in cluster 1 moving with the long way was stable firstly and then rose slightly. Thereafter, it declined dramatically. Regarding winter, the range of initial heights was the smallest among four seasons. And all trajectories had the transport height decreased gradually regardless of cluster. It should be noted that the press profiles were not related with the concentrations of PM in trajectories regardless of season.

[Fig. 7 Pressure profile of back trajectories for air flow in Hefei City between 2018 and 2020]

3.3 Potential contributor sources identification

3.3.1PSCF analysis

WPSCF maps for PM_{10} and $PM_{2.5}$ of Hefei City between 2018 and 2020 are provided in Figs. 8 and 9.

[Fig. 8 WPSCF maps for PM10 of Hefei City between 2018 and 2020]

[Fig. 9 WPSCF maps for PM2.5 of Hefei City between 2018 and 2020]

In Spring, PM_{10}'s WPSCF over 0.60 were mainly located in two large zones from 10 provinces (Anhui, Hubei, Hunan, Jiangxi, Zhejiang, Guangxi, Henan, Shanxi, Shaanxi and Huhhot). And the main potential contributors of atmospheric PM_{10} in Heifei were distributed in the neighboring region of Anhui, Jiangxi and Zhejiang, the middle north of Fujian, the border of Hunan and Hubei, the middle east and south of Hubei, the middle north of Hunan, the border of Shanxi and Henan, etc. Otherwise, the area and value of WPSCF for $PM_{2.5}$ were smaller than that of PM_{10} in spring. The significant contributors came from the northeast of Jiangxi, the junction of Anhui, Jiangxi and Zhejiang, the north of Fujian and the northeast of Guangxi, which also could contribute PM_{10} considerably to Hefei.

In summer, the value of WPSCF, exceeding 0.70, for PM_{10} mainly appeared in Anhui, Jiangsu and Zhejiang province. And the major cities included Tongling, Xuancheng, Wuhu and Huangshan in Anhui province, Changzhou, Wuxi and Suzhou in Jiangsu province and Huzhou, Jiaxing, Shaoxing, Hangzhou, Quzhou, Jinhua, Lishui in Zhejiang province. Moreover, there were several patches from Jiangxi, Fujian, Shandong and Henan province with WPSCF as 0.70–0.80, being the significant potential contributor. Comparatively, $PM_{2.5}$'s WPSCF was mainly within the range of < 0.70. And the places, away from the southeast of Hefei, including Tongling, Chizhou, Wuhu, Xuancheng in Anhui province and Huzhou and Hangzhou in Zhejiang Province were recognized as the considerable contributors of $PM_{2.5}$.

As shown in Fig. 8(c), the sources likely affecting Heifei' PM_{10} scattered in Huangshi, Ezhou, Huanggang, Xianning, Suizhou, Jingmen, Shiyan, Nanyang, Sanmenxia, Shangluo,Weinan, Yanan, Yulin and Qingyang Cities. Moreover, there were large areas with WPSC between 0.50 and 0.60 from the middle-lower Yangtze Plain, the Northeast Plain, the Loess Plateau and the Inner Mongolian Plateau. As to $PM_{2.5}$, its major contributors were from southern Hubei (Xianning and Huanggang) and western Jiangxi (Jiujiang, Yichun and Xinyu). Additionsally, Huaibei, Shangluo, Sanmenxia and Qingyang can also be considered as the significant contributor.

Within winter, WPSC values both of PM_{10} and $PM_{2.5}$ the highest of four seasons. The area of PM's contributors to Hefei was remarkably increased. And the contribution was stronger in northern China than southern China. Specifically, the contributors of PM_{10} were mainly seated at west, northwest and southwest of Hefei city. The places, between the line of Yinchuang-Zhengzhou city and the line of Zhongwei-Pingdingshan city, covering Henan, Shanxi, Shaanxi and Gansu province, were found to be the significant contributor of PM_{10} with the largest area. Moreover, northeast Hubei province, southeastern Hubei province, Jianghan Plain and northeast Hunan province were also the strong contributor. On the other hand, $PM_{2.5}$ was mainly contributed by southeastern Shandong, eastern Henan, northern Anhui, southeastern Hubei, northeast Hunan and southern Shanxi.

3.3.2 WCWT analysis

Figure 10 shows WCWT map distributions of PM_{10}. The results were very similar to that of WPSCF method. In spring the areas with WCWT over 100 $\mu g \cdot m^{-3}$ covering the border of Shanxi and Shaanxi province (Lvliang, Linfen, Yulin and Yanan city), the border of Shanxi and Henan province (Yuncheng, Jincheng, Sanmenxia, Jiyuan, Luoyang and Jiaozuo city), the middle of Henan province (Zhengzhou, Xuchang and Pingdingshan city), the center of Hebei province (Boding city), the junction of Anhui, Jiangxi and Zhejiang province (Huangshan Jingdezheng, Shangrao and Quzhou city). In summer, WCWT was observed in the range of < 70 $\mu g \cdot m^{-3}$. And the places of the south of Anhui province, the south of Jiangsu province and the middle and northern west of Zhejiang province were identified as the main potential contributor. Otherwise, during autumn WCWT of 100–157 $\mu g \cdot m^{-3}$ was found mainly in Henan and Hubei province. Moreover, several patches from Anhui, Shanxi and Shaanxi province were also the significant contributor of PM_{10}. Over winter, there an enormous region with WCWT of PM_{10} over 90 $\mu g \cdot m^{-3}$. The major contributors were located almost within the whole of Henan province, the middle east of Hubei province, large area of Anhui province, the southwest of Shanxi province, the southwest of Shandong province, west of Zhejiang province, the neighboring region of Hubei, Hunan and Guangxi province as well as the middle of Guangxi province.

[Fig. 10 WCWT maps for PM10 of Hefei City between 2018 and 2020]

WCWT distribution of $PM_{2.5}$ is given in Fig. 11. The main contributors of $PM_{2.5}$ with WCWT > 40 $\mu g \cdot m^{-3}$ were widely distributed in the central and eastern China. And the neighboring region of Anhui with Jiangxi and Zhejiang Province, the northwest part of Henan Province, and the middle, northwest and east places of Shandong Province were observed to contribute WCWT as 50 ~ 60 $\mu g \cdot m^{-3}$. Comparatively, summer had the smallest $PM_{2.5}$ WCWT (< 40 $\mu g \cdot m^{-3}$) among four seasons. And, the areas with WCWT higher than 30 $\mu g \cdot m^{-3}$ were within the large region of southern Anhui province, the north of Zhejiang province and the south of Jiangsu province. Into autumn, the contribution area of $PM_{2.5}$ started to expand with WCWC mainly as 40 ~ 70 $\mu g \cdot m^{-3}$. Over winter, WCWT of 90 ~ 100 $\mu g \cdot m^{-3}$ was concentrated at the southeast of Hubei Province, the east of Henan Province and the southwest of Shandong Province.

[Fig. 11 WCWT maps for PM2.5 of Hefei City between 2018 and 2020]

As above-discussed, the potential contributor sources to Hefei city seasonally varied. And the places from Shanxi, Hebei, Henan and Anhui Province were identified as the major contributor. Dring 2001 ~ 2005, dust storm episode could significantly affect Hefei's PM concentration, especially in spring [22]. Interestingly, inner Mongolia where dust storm episode frequently previously did not seem to be the important contributor by the present study. A study by Yu et al. [23] shows that Anqing, a neighboring city of Hefei, was mainly contributed by the sources from the east of Hubei province, north of Jiangxi province and south of Hunan province, which was coupled with a planar area involved in Shanxi, Henan, southern Shandong and northern Anhui province. And there are several places as the same contributor to both Anqing and Hefei.

Conclusion

In the present study, transport pathway and potential contributor sources of particulate matter in Hefei City during 2018 ~ 2020 were identified. The pollution level of particulate matter in Hefei City had been decreased considerably but still was unfavorable. PM_{10} and $PM_{2.5}$ had the highest concentration in winter while the lowest in summer. The comparation with pervious study shows that the relationship between PM_{10} and $PM_{2.5}$ had been weakened by a small margin, indicating the pollution sources of particulate matter had changed slightly. And the seasonal variation of $PM_{2.5}/PM_{10}$ shows that the atmospheric pollution type of Hefei by particulate matter in winter may be different from that of other seasons. During spring, autumn and winter, Hefei was mainly affected by landlocked air mass derived from either north China or northwest China. The trajectories passed Fen-Wei Plain and '2 + 26' City had high PM concentration. Spatiotemporal distribution of backjectories' pressure profile suggests that the influence of near surface air mass was stronger in summer. Except for summer, the places from Shanxi, Hebei, Henan and Anhui Province were identified as the major contributor.

Declarations

Acknowledgements

This reseaerch was supported by the Open Fund by Jiangsu Key Laboratory of Atmospheric Environment Monitoring and Pollution Control, the Project Funded by the Priority Academic Program Development of

Jiangsu Higher Education Institutions (PAPD) and the Scientific Research Foundation for the Returned Overseas Chinese Scholars of Anhui Province. The authors are grateful for the support.

Author Declarations

1. Ethics Declaration statement

Not applicable

2. Consent to Participate

Not applicable

3. Consent for publication

Not applicable

Funding

This work was supported by [Nanjing University of Information Science & Technology and the Human Resources and Social Security Department of Anhui Province]. Author Siping Niu has received research support from Nanjing University of Information Science & Technology and the Human Resources and Social Security Department of Anhui Province.

Competing Interests

The authors declare that The authors have no relevant financial or non-financial interests to disclose.

Author Contributions

Siping Niu: Conceptualization, Methodology, writing, Reviewing and Editing. Tiantian Wang: Data collection and analysis. Jianghua Yu: Reviewing. All authors read and approved the final manuscript.

Data Availability

The datasets generated and analyzed during the current study are available from the corresponding author on reasonable request.

References

1. Han, L., Zhou, W., Li, W., & Qian, Y. (2018). Urbanization strategy and environmental changes: An insight with relationship between population change and fine particulate pollution. Sci. Total. Environ, 642, 789–799.
2. Wei, G., Zhang, Z., Ouyang, X., Shen, Y., Jiang, S., Liu, B., & He, B. (2021). Delineating the spatial-temporal variation of air pollution with urbanization in the Belt and Road Initiative area. Environ

Impact Assess Rev, 91, 106646.

3. Shi, Y., Bilal, M., Ho, H.C., & Omar, A. (2020). Urbanization and regional air pollution across South Asian developing countries–A nationwide land use regression for ambient $PM_{2.5}$ assessment in Pakistan. Environ. Pollut, 266, 115145.
4. Luo, X., Sun, K., Li, L., Wu, S., Yan, D., Fu, X., & Luo, H. (2021). Impacts of urbanization process on $PM_{2.5}$ pollution in “2 + 26” cities. J. Clean. Prod, 284, 124761.
5. Adam, M.G., Tran, P.T., Bolan, N., & Balasubramanian, R. (2020). Biomass burning-derived airborne particulate matter in Southeast Asia: A critical review. J. Hazard. Mater, 407, 124760.
6. Oliveira, M., Delerue-Matos, C., Pereira, M.C., & Morais, S. (2020). Environmental Particulate Matter Levels during 2017 Large Forest Fires and Megafires in the Center Region of Portugal: A Public Health Concern? Int. J. Environ. Res. Public Health, 17 (3), 1032.
7. Wang, J., & Du, P. (2021). Quarterly $PM_{2.5}$ prediction using a novel seasonal grey model and its further application in health effects and economic loss assessment: evidences from Shanghai and Tianjin, China. Nat. Hazards, 107 (1), 889–909.
8. Ban, J., Ma, R., Zhang, Y., & Li, T. (2021). $PM_{2.5}$-associated risk for cardiovascular hospital admission and related economic burdens in Beijing, China. Sci. Total. Environ, 799, 149445.
9. Liu, L., Duan, Y., Li, L., Xu, L., Yang, Y., & Cu, X. (2020). Spatiotemporal trends of $PM_{2.\,5}$ concentrations and typical regional pollutant transport during 2015–2018 in China. Urban Clim, 34 (8), 100710.
10. Zhao, N., Wang, G., Li, G., & Lang, J. (2021). Trends in Air Pollutant Concentrations and the Impact of Meteorology in Shandong Province, Coastal China, during 2013–2019. Aerosol. Air Qual. Res, 21, 200545.
11. MOEE (Ministry of Ecology and Environment of the people’s Republic of China) 2021. https://www.mee.gov.cn/hjzl/sthjzk/zghjzkgb/202105/P020210526572756184785.pdf (accessed on 27 September 2021).
12. Gustin, M.S., Dunham-Cheatham, S.M., Zhang, L., Lyman, S., & Castro, M. (2021). Use of membranes and detailed HYSPLIT analyses to understand atmospheric particulate, gaseous oxidized, and reactive mercury chemistry. Environ. Sci. Technol, 55 (2): 893–901.
13. Ma, Y., Wang, M., Wang, S., & Wu, K. (2021). Air pollutant emission characteristics and HYSPLIT model analysis during heating period in Shenyang, China. Environ. Monit. Assess, 193 (1): 1–14.
14. Olise, F.S., Ogundele, L.T., Olajire, M.A., & Owoade, O.K. (2020). Seasonal Variation, pollution indices and trajectory modeling of bio-monitored airborne particulate around two smelting factories in Osun State, Nigeria. Aerosol Sci Eng, 4 (4), 260–270.
15. Singh, A., Srivastava, A.K., Varaprasad, V., Kumar, S., Pathak, V., & Shukla, A.K. (2021). Assessment of near-surface air pollutants at an urban station over the central indo-Gangetic Basin: role of pollution transport pathways. Meteorol. Atmos. Phys, 133, 1127–1142.
16. Liu, S., Hua, S., Wang, K., Qiu, P., Liu, H., Wu, B., & Tian, H. (2018). Spatial-temporal variation characteristics of air pollution in Henan of China: Localized emission inventory, WRF/Chem

simulations and potential source contribution analysis. Sci. Total. Environ, 624, 396–406.

17. Hao, T., Cai, Z., Chen, S., Han, S., Yao, Q., & Fan, W. (2019). Transport pathways and potential source regions of $PM_{2.5}$ on the west coast of Bohai Bay during 2009–2018. Atmosphere, 10 (6), 345.
18. Li, H., He, Q., & Liu, X. (2020). Identification of Long-Range Transport Pathways and Potential Source Regions of $PM_{2.5}$ and PM_{10} at Akedala Station, Central Asia. *Atmosphere*, 11 (11), 1183.
19. Li, D., Liu, J., Zhang, J., Gui, H., & Cheng, Y. (2017). Identification of long-range transport pathways and potential sources of $PM_{2.5}$ and PM_{10} in Beijing from 2014 to 2015. J. Environ. Sci, 56 (6), 214–229.
20. Luo, B., Liu, X., & Management, S.O. (2019). Investigation on the source of air pollutants in hefei city based on backward trajectory model. Journal of University of Science and Technology of China, 49 (4), 321–328.
21. Shen, S. (2019). Study on the characteristics of $PM_{2.5}$ pollution and its transportation path in typical cities of Anhui Province. Master thesis, Hefei University of Technology.
22. Shi, C., Yao, Y., Zhang, P., & Qiu, M. (2008). Classification of PM_{10} transport trajectory in Hefei. PLATEA U METEORO LOGY, 27 (6), 1383–1391.
23. Yu, G., Li, F., & Han, C. (2017). Trajectory analysis of atmospheric long range transport of particles in Anqing City. Resources and Environment in The Yangtze Basin, *26*(12),2111–2119.

Figures

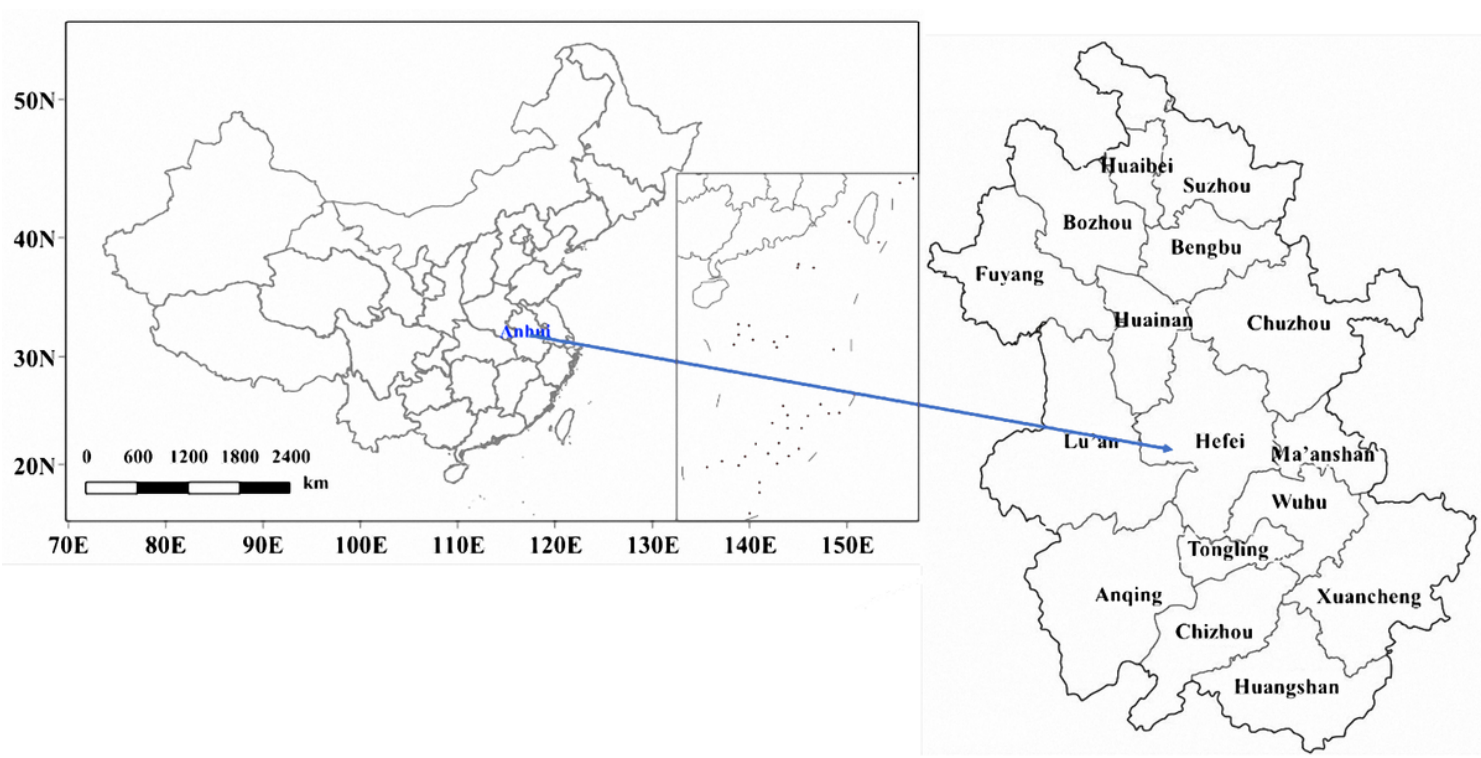

Figure 1

Location of Hefei City

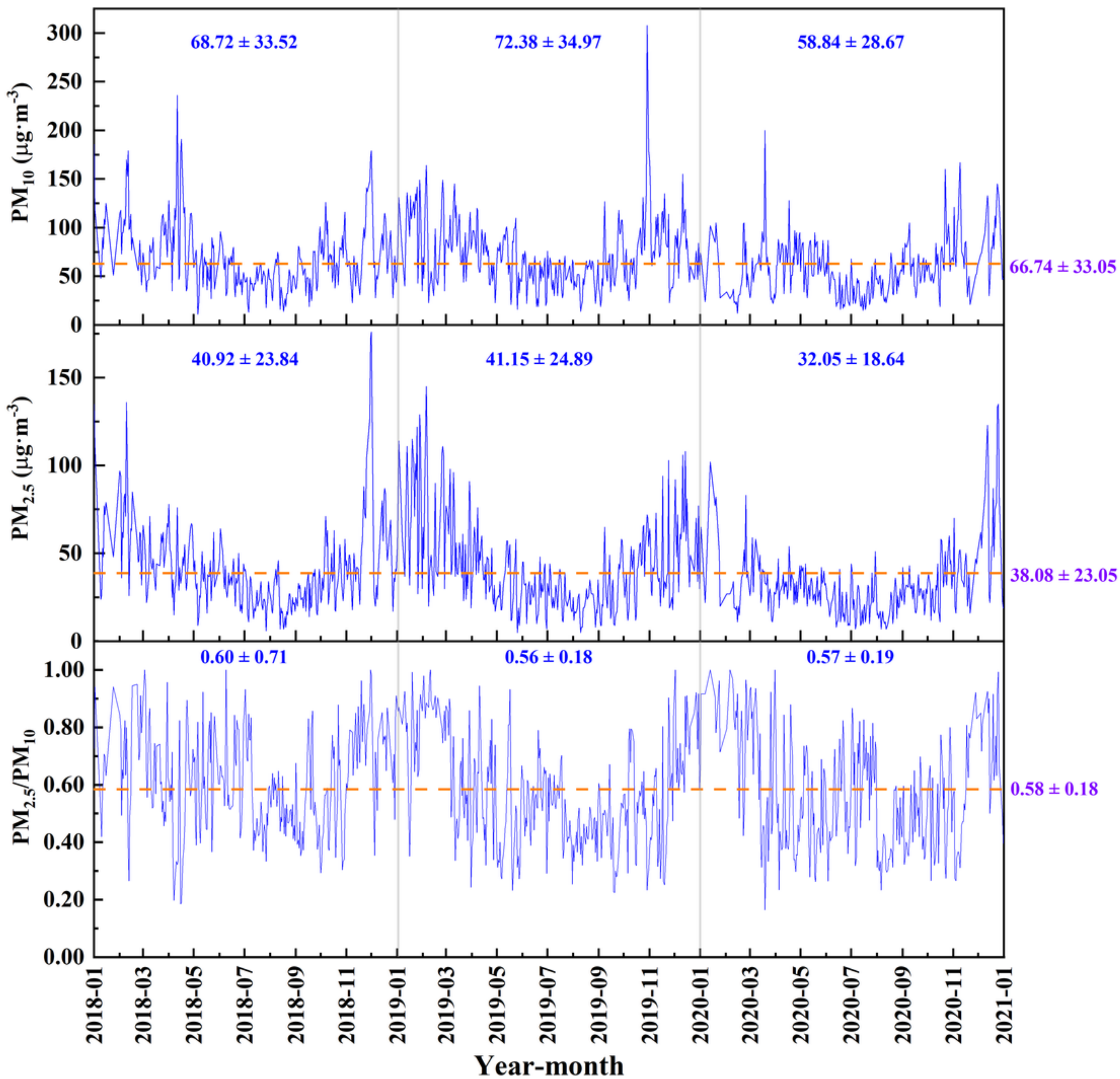

Figure 2

Daily variation of particulate matter in Hefei city between 2018 and 2020

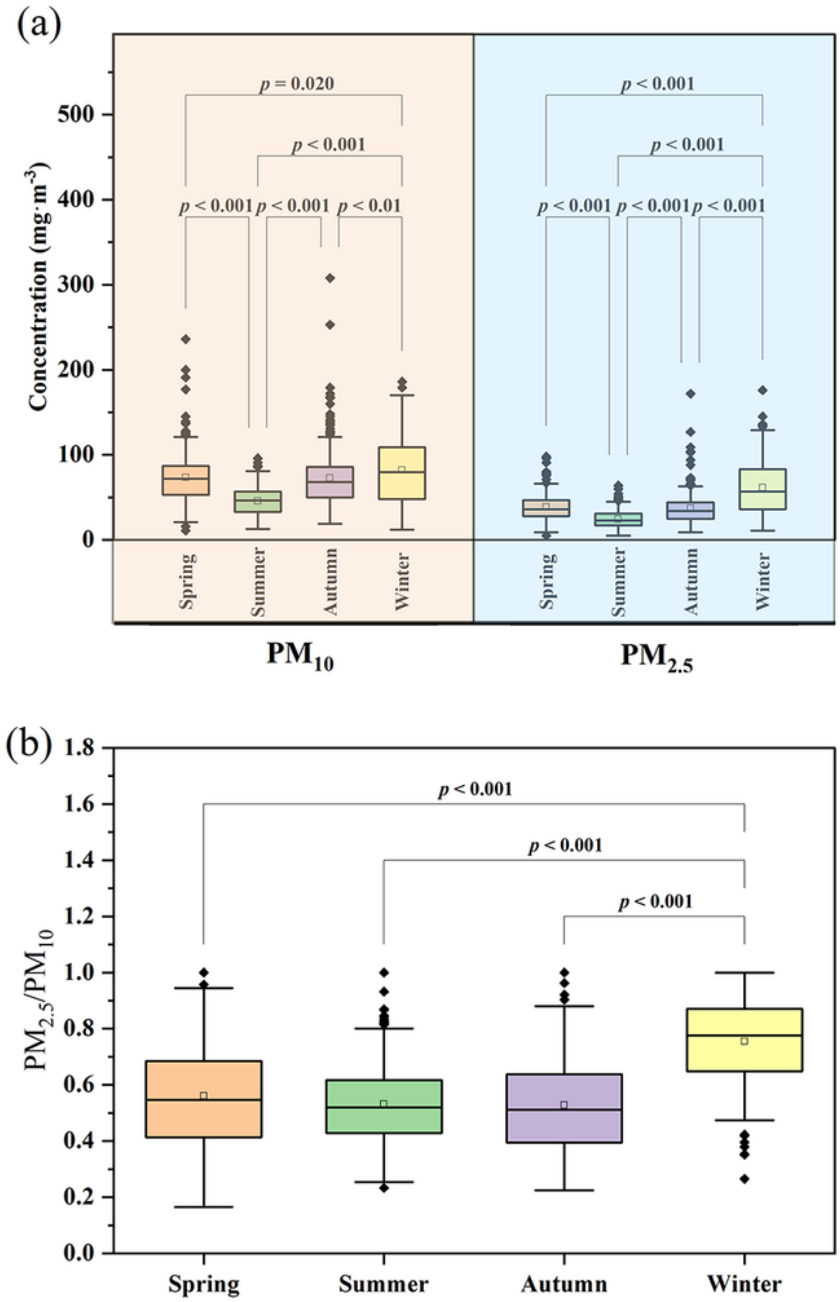

Figure 3

Seasonal variation of particulate matter in Hefei city between 2018 and 2020

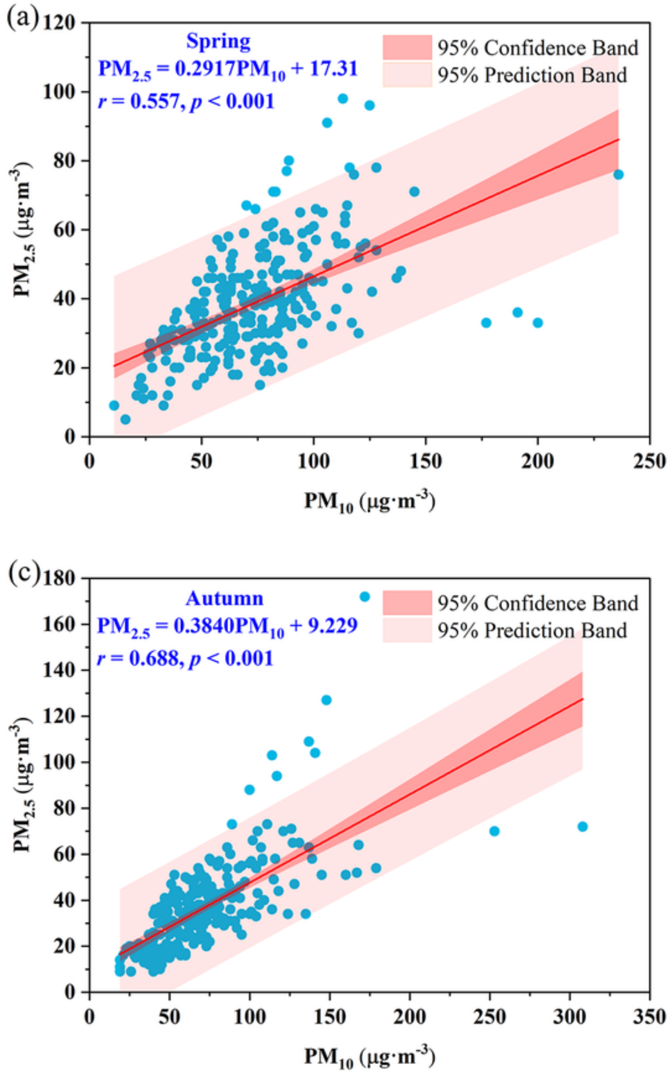

Figure 4

Correlationship between PM_{10} and $PM_{2.5}$ with respect to season n Hefei city between 2018 and 2020

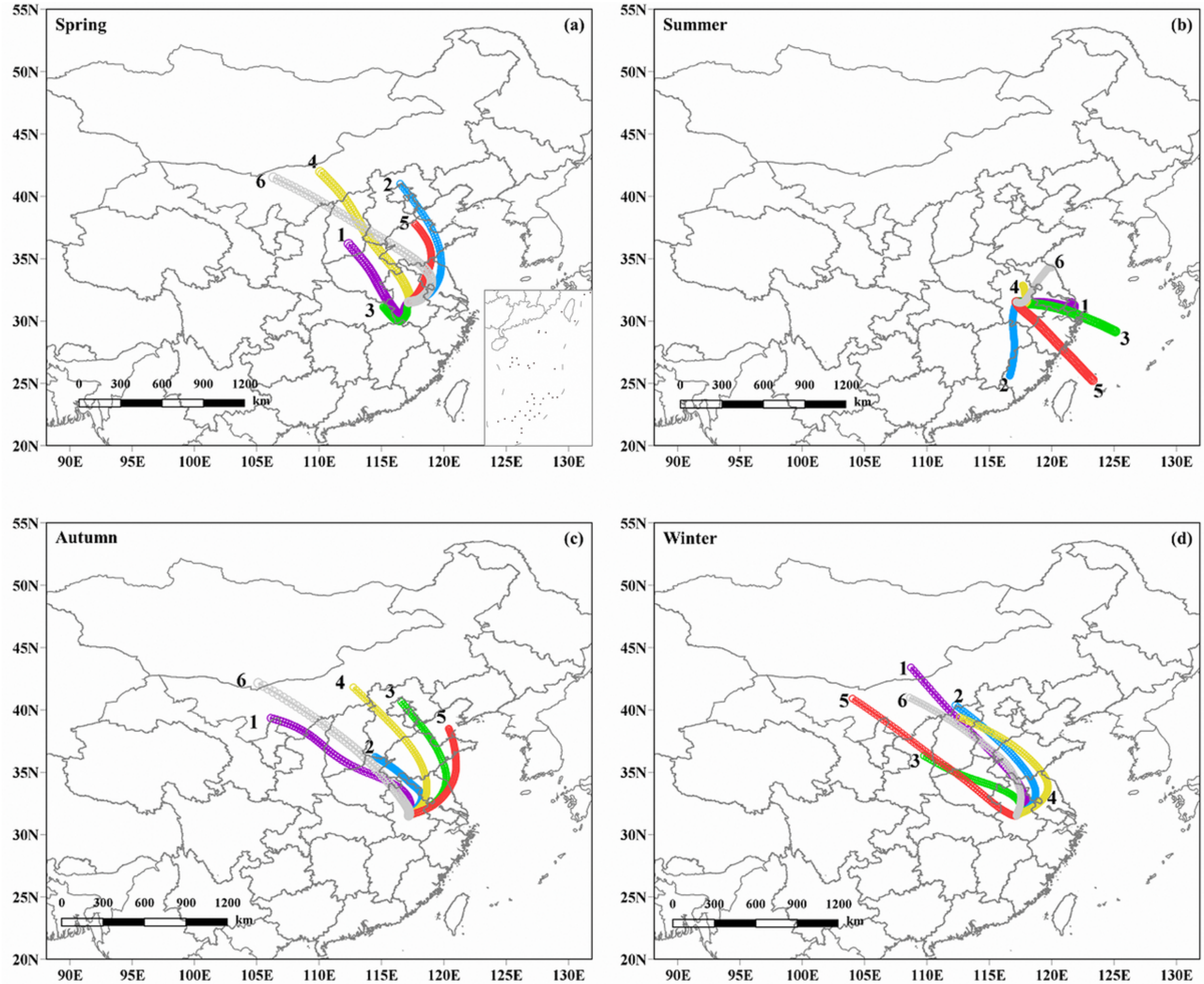

Figure 5

Clusters of back trajectories of air flow for Hefei City between 2018 and 2020

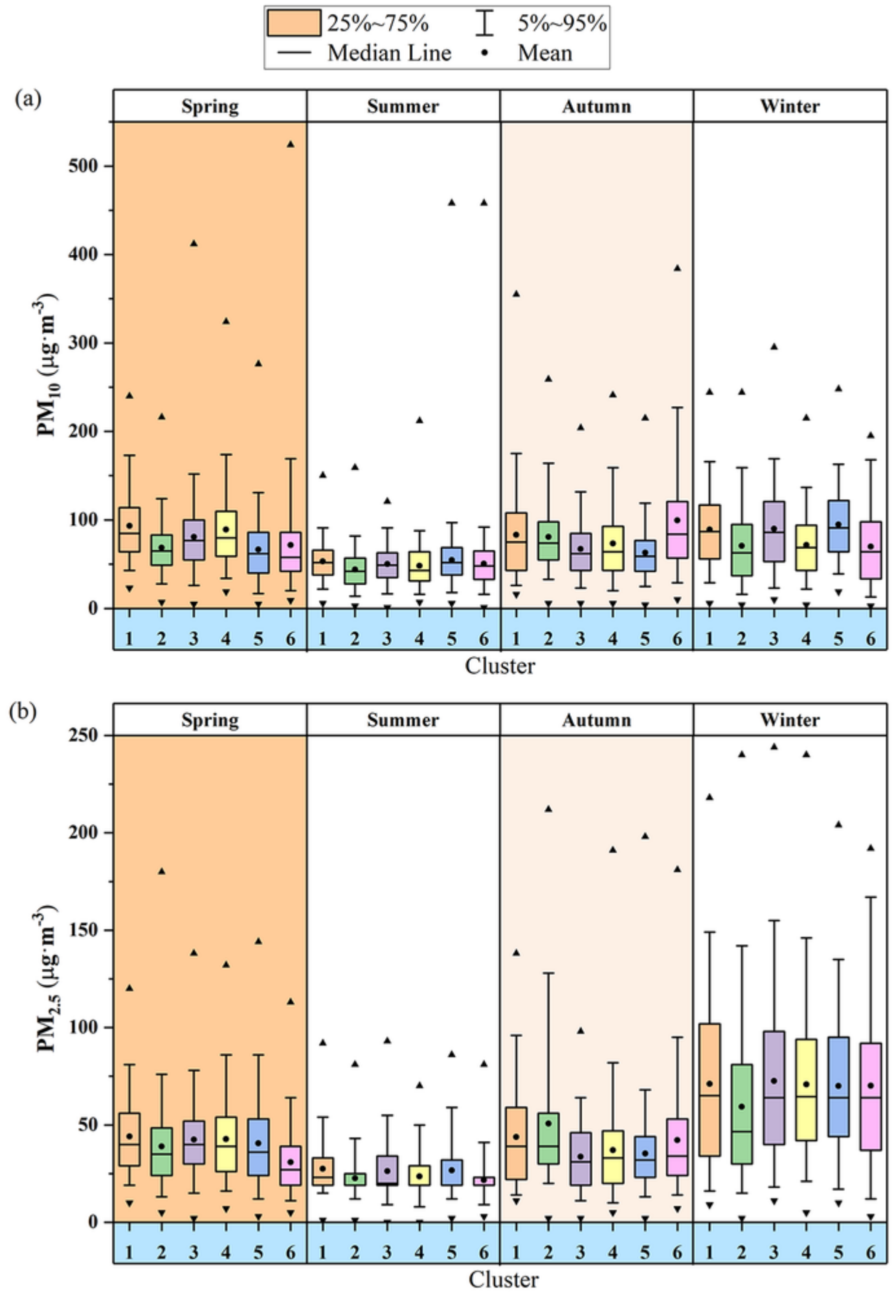

Figure 6

PM_{10} and $PM_{2.5}$ portioned by trajectory cluster of air flow for Hefei City between 2018 and 2020

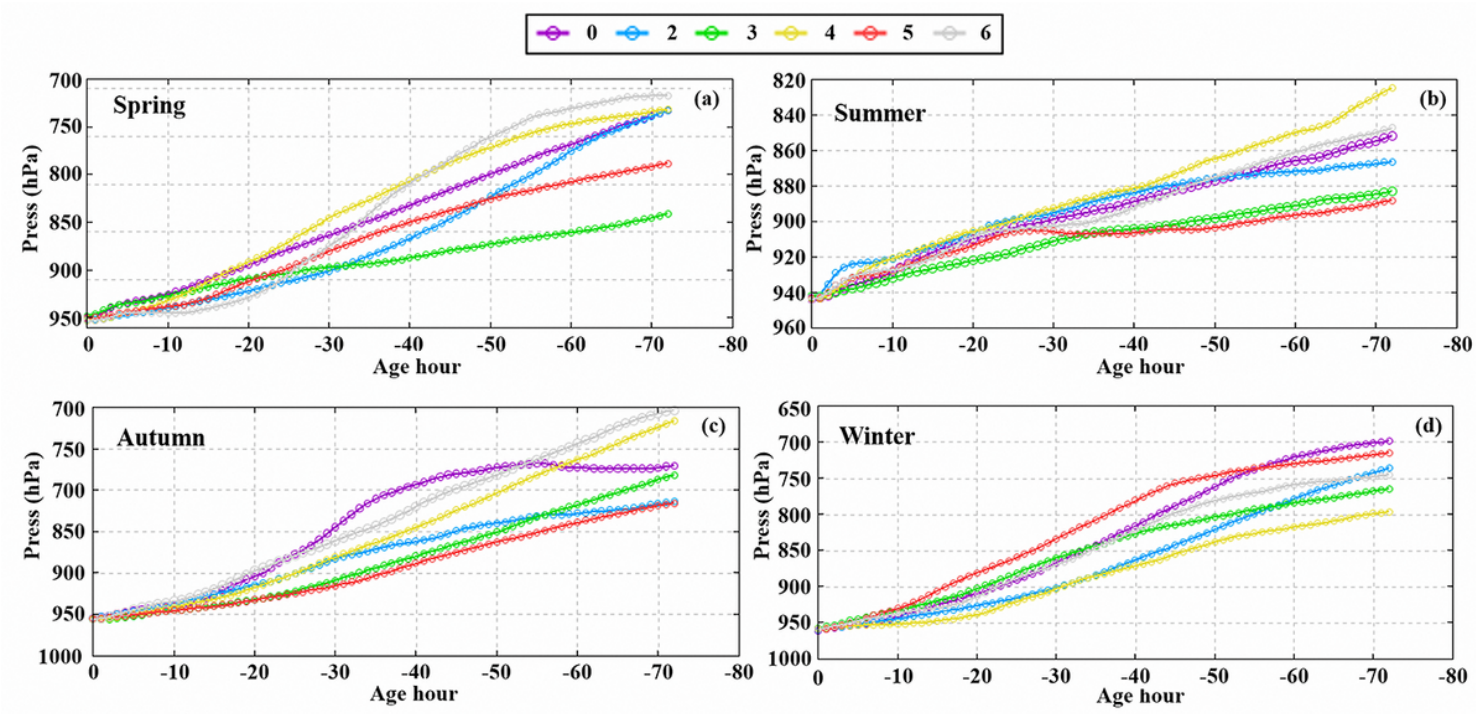

Figure 7

Pressure profile of back trajectories for air flow in Hefei City between 2018 and 2020

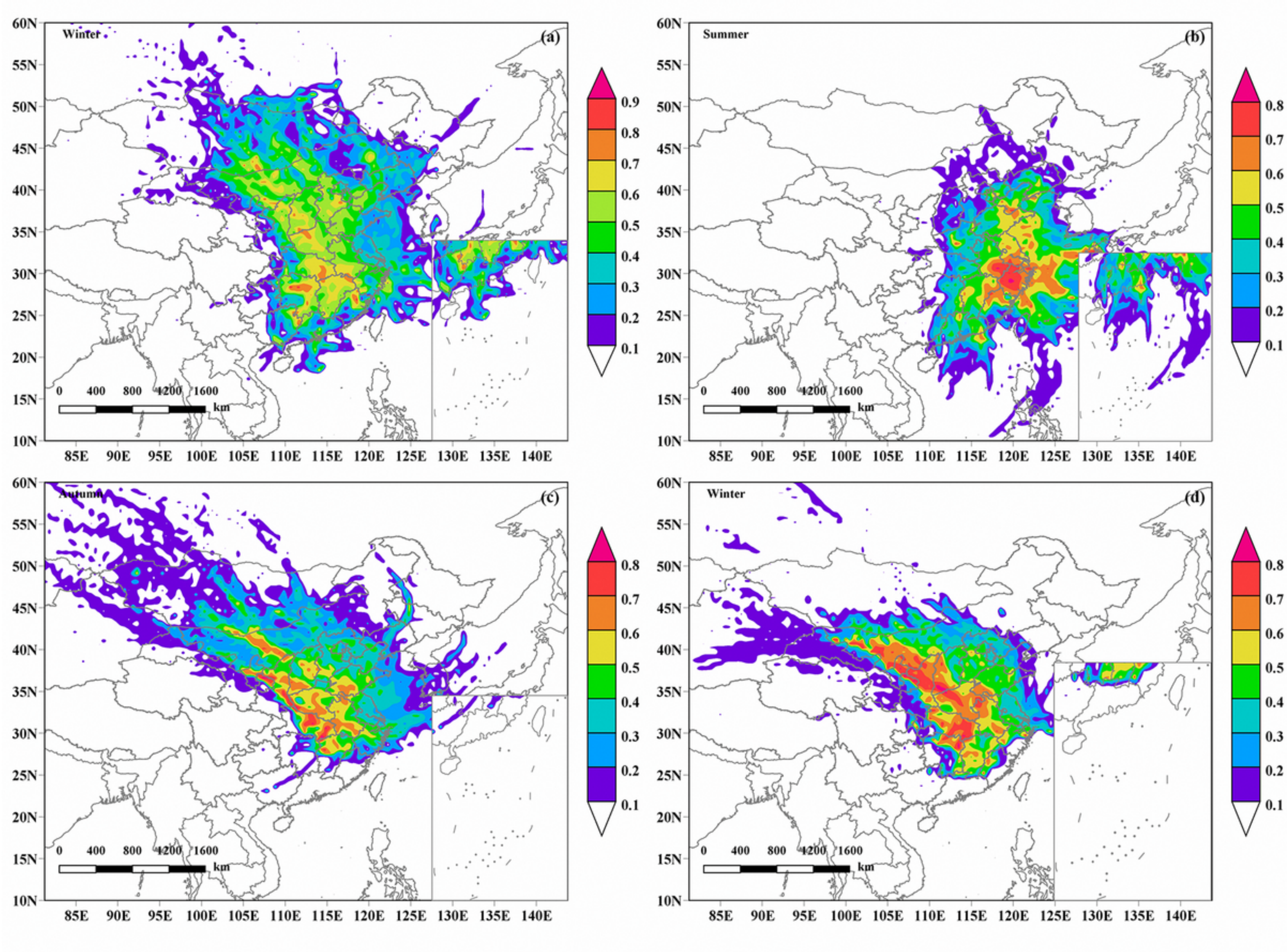

Figure 8

WPSCF maps for PM10 of Hefei City between 2018 and 2020

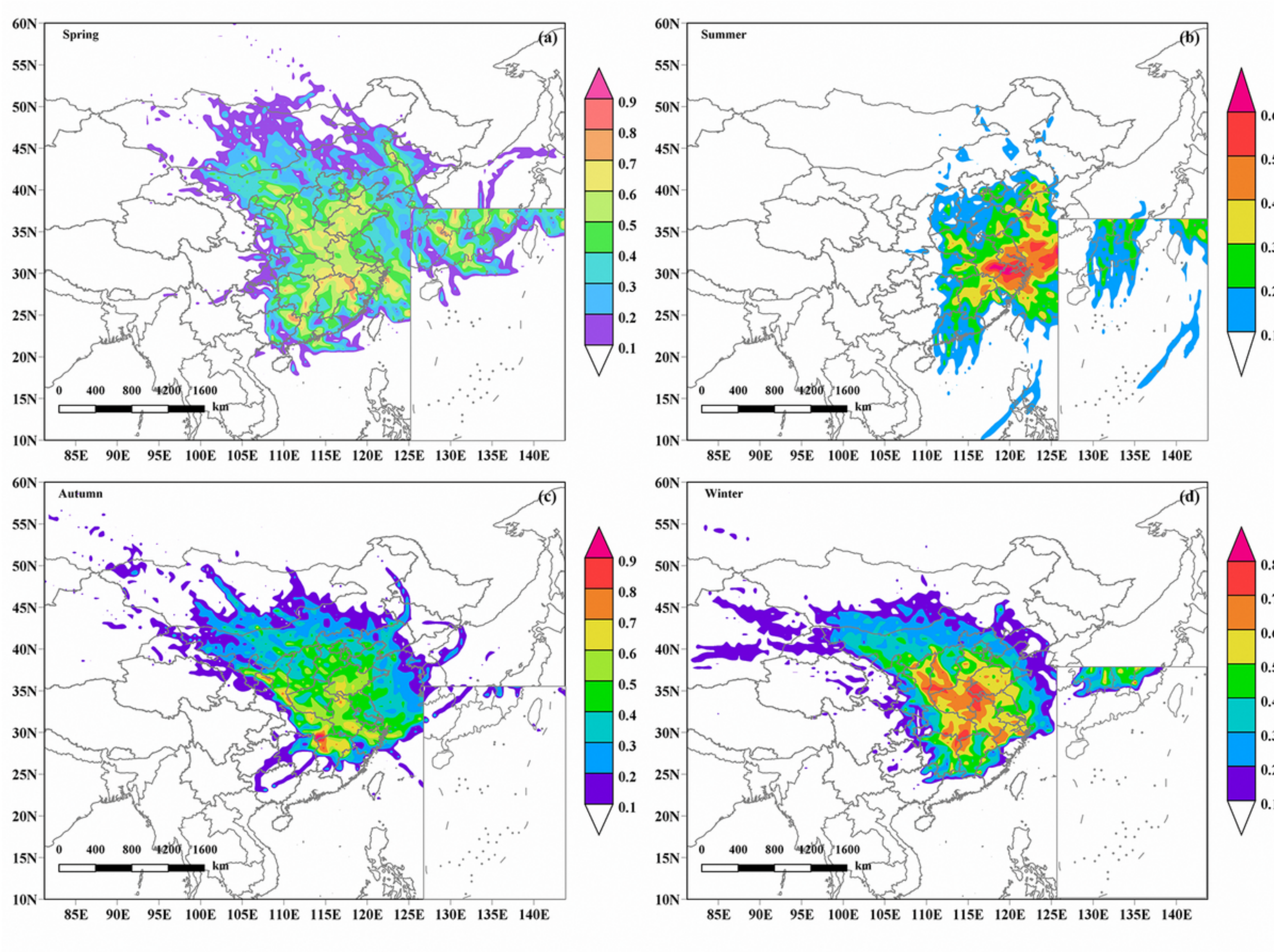

Figure 9

WPSCF maps for PM2.5 of Hefei City between 2018 and 2020

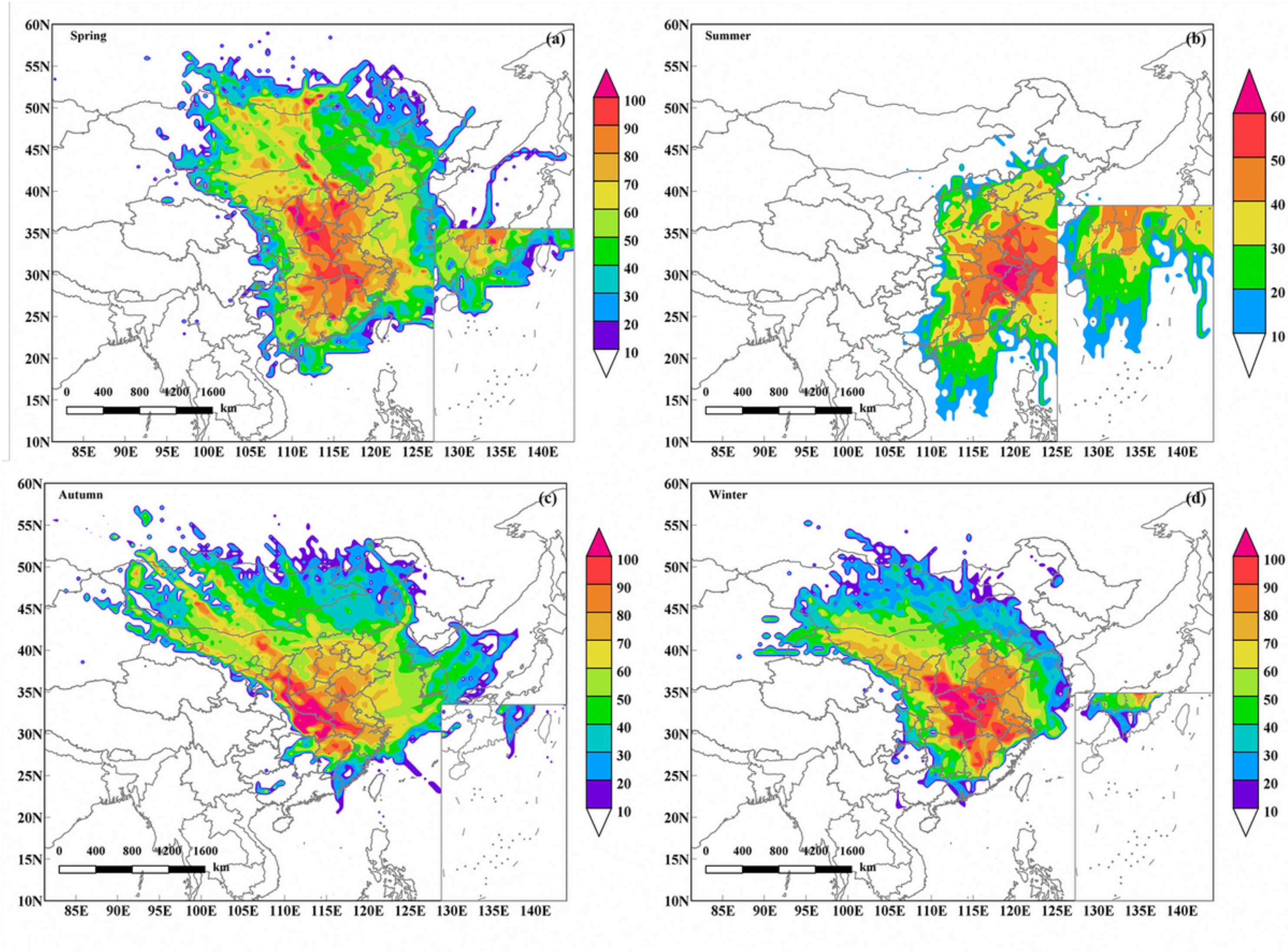

Figure 10

WCWT maps for PM10 of Hefei City between 2018 and 2020

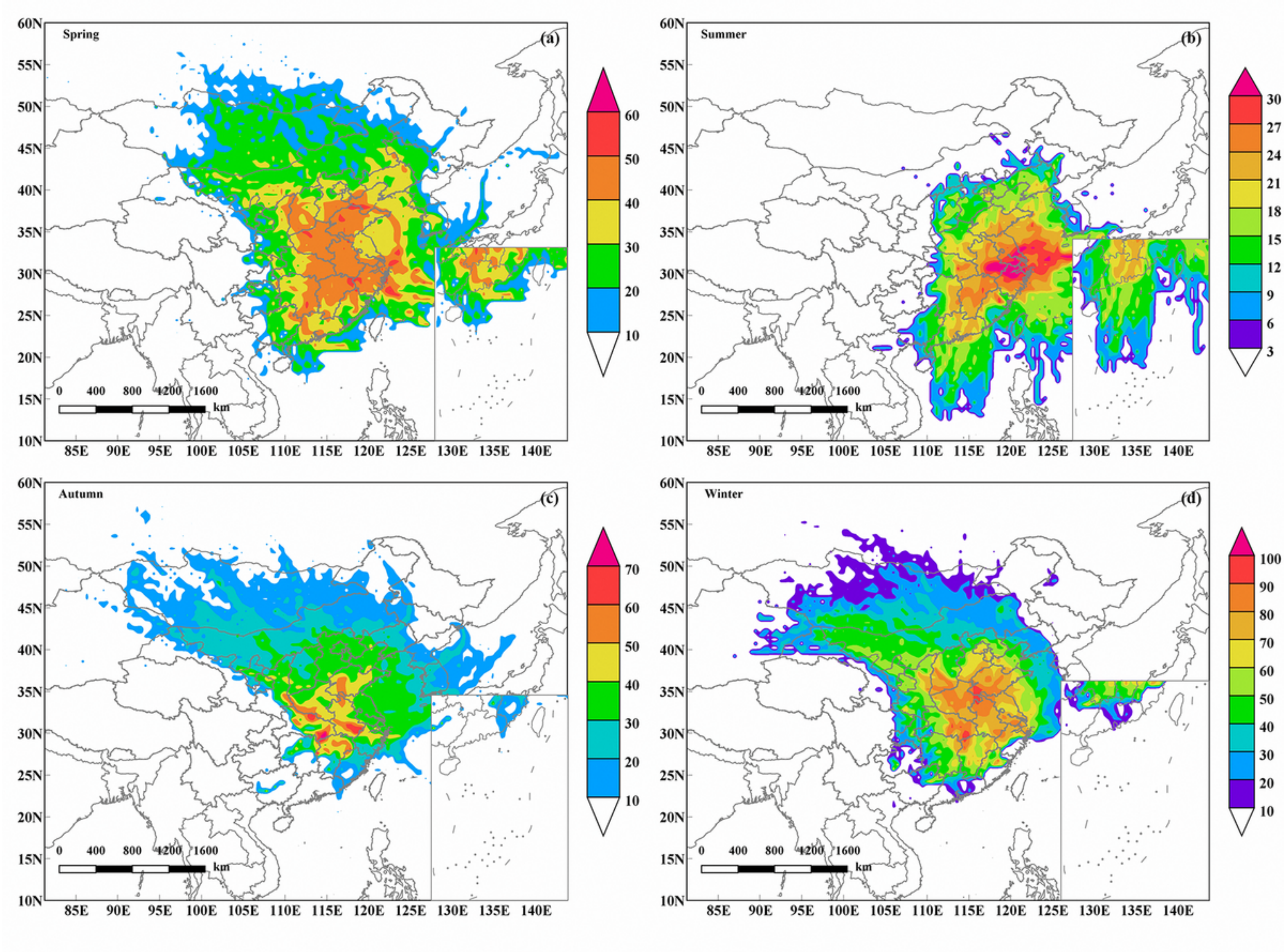

Figure 11

WCWT maps for PM2.5 of Hefei City between 2018 and 2020